


 Cite this: *Phys. Chem. Chem. Phys.*, 2025, 27, 6845

 Received 9th November 2024,  
Accepted 19th March 2025

DOI: 10.1039/d4cp04279d

rsc.li/pccp

## Influence of light on ad- and desorption processes on titanium dioxide surfaces towards efficient CO<sub>2</sub> photoreduction†

 Pawel Naliwajko,<sup>a</sup> Nikolaos G. Moustakas,<sup>a</sup> Marcus Klahn,<sup>a</sup> Tim Peppel<sup>id</sup><sup>a</sup> and Jennifer Strunk<sup>id</sup><sup>\*ab</sup>

**This work addresses the often-overlooked effect of light-induced sorption behavior of CO<sub>2</sub> on powder TiO<sub>2</sub> surfaces, as potential first step to photocatalytic CO<sub>2</sub> activation. These investigations will lead to a more detailed understanding of the light-induced chemistry of CO<sub>2</sub> on TiO<sub>2</sub>, to eventually unravel the CO<sub>2</sub> photoreduction mechanism.**

### Introduction

While anthropogenic carbon dioxide (CO<sub>2</sub>) provides a major contribution to the climate crisis, at the same time it offers a virtually endless feedstock of carbon. Through photocatalytic reduction of CO<sub>2</sub>, solar energy can be stored in the form of chemical bonds of valuable platform chemicals and fuels leading to a simultaneous combating of climate change and the energy crisis. In photocatalytic CO<sub>2</sub> reduction (and in photocatalysis in general), a photocatalyst needs to serve a double role: that of photoabsorber and that of substrate for the reactants to adsorb and react. Many studies focus on the photo-absorbing role of the photocatalyst neglecting the very important sorption processes occurring at the surface of the material. While those are usually very well understood in the dark, in particular for single crystals,<sup>1,2</sup> significant changes in the electronic structure of the light-absorbing substrate might occur under light irradiation. Sorption processes are often considered to be rate-limiting steps in heterogeneous catalytic reactions.<sup>3</sup> In most cases the photocatalytic conversion rates of CO<sub>2</sub> to e.g., methane (CH<sub>4</sub>) are in the order of a few μmol g<sub>cat</sub><sup>-1</sup> h<sup>-1</sup>, mostly due to high thermodynamic stability of CO<sub>2</sub>. As the

elementary steps in the reaction mechanism are still only partly understood, directed improvements to the photocatalysts are difficult. Titanium dioxide (TiO<sub>2</sub>), particularly in its commercially available form P25 (a mixture of anatase and rutile in an 80 : 20 ratio, Evonik Industries) is the most studied metal oxide in photocatalysis including CO<sub>2</sub> photoreduction. From its polymorphs (anatase, rutile and brookite), anatase is considered to be the most active one in many photocatalytic applications.<sup>4</sup> Many works have attempted to study the mechanism of CO<sub>2</sub> reduction on TiO<sub>2</sub>-based materials with IR spectroscopy,<sup>5,6</sup> but due to the complicated reaction conditions and band overlap, the assignments varied greatly. Thus, we took a step back and simplified the system by looking only at the adsorption. It is known from our previous studies<sup>7</sup> that stable carbonate species formed upon CO<sub>2</sub> adsorption in the dark are likely not relevant but detrimental for product formation in photocatalytic CO<sub>2</sub> reduction. Other species may be more relevant reaction intermediates. In the current work, the sorption behavior of CO<sub>2</sub>, in the dark and under light irradiation, on TiO<sub>2</sub> (P25 and pure anatase) was studied by means of diffuse reflectance FT-IR spectroscopy (DRIFTS). DRIFTS allows the investigation of the formation of molecular species (e.g., carbonates) on the surface of TiO<sub>2</sub> under the influence of light, simulating reaction conditions thus providing valuable insights into the underlying CO<sub>2</sub> photoconversion mechanism.

### Experimental

All FT-IR measurements were performed on a Nicolet iS50R Advanced FT-IR spectrometer manufactured by Thermo Scientific. It was equipped with a Polaris™ high stability, long lifetime mid-IR source, a KBr beam guide, and a liquid nitrogen cooled MCT-B detector allowing measurements in the range from 12 000 to 400 cm<sup>-1</sup> with a resolution of > 0.1 cm<sup>-1</sup>. DRIFTS measurements were performed utilizing an *in situ* high temperature reaction chamber equipped with a Praying Mantis™ mirror array

<sup>a</sup> Leibniz Institute for Catalysis (LIKAT), Albert-Einstein-Str. 29a, 18059 Rostock, Germany

<sup>b</sup> Technical University of Munich (TUM), Lichtenbergstr. 4, 85748 Garching b. München, Germany. E-mail: jennifer.strunk@tum.de

† Electronic supplementary information (ESI) available. See DOI: <https://doi.org/10.1039/d4cp04279d>



(Harrick HVC-DRP-5, Fig. S1, ESI†). It featured a stainless-steel sample holder and hemispherical stainless-steel dome with metal circular rim and three windows of which two were made of KBr and one of quartz. The quartz window was UV-transparent allowing irradiation of the samples in the optical range. The powdered sample was filled in the sample holder in the center of the chamber, over a fine metallic mesh (100  $\mu\text{m}$  pore size). The respective gas ( $\text{CO}_2$  or Ar) was passed through the side channel of the chamber and exiting through the channel beneath the sample providing optimal gas–solid interaction. A flow rate of 30  $\text{ml min}^{-1}$  was chosen for all gases. The bottom part and the sample holder of the measurement cell was temperature controlled using water for cooling and the build-in heat cartridges for heating, regulated by a Harrick ACT/low voltage heating control element based on the Watlow EZ-ZONE© dual channel controller. Photos of the setup are presented in Fig. S2 (ESI†).

All spectra were recorded in the spectral range from 4000 to 400  $\text{cm}^{-1}$  with a resolution of 4  $\text{cm}^{-1}$  and averaging 200 scans, resulting in one spectrum every 1.3 min. All changes in the reaction system *e.g.*, changing of temperature or gas composition, addition of light *etc.* were implemented after recording at least one spectrum. With this a baseline spectrum was available for post-processing of the recorded series of spectra and creation of subtraction (difference) spectra which offer a better visibility of changes in the spectra. A LUMATEC Superlite S04 lamp (Fig. S3, ESI†) equipped with a flexible light conductor was used to illuminate the samples with UV light (range: 320–400 nm, light intensity: 135  $\text{mW cm}^{-2}$ ).

The experimental procedure consisted of three main parts: (i) pre-treatment, (ii)  $\text{CO}_2$  adsorption and (iii) post-treatment. A schematic depiction of the experimental procedure can be found in Fig. S4 (ESI†). After introduction of the sample, the reaction chamber was purged with Ar for 2 h to remove all residual air. Each sample was heated in a steady Ar flow up to 725 K with a heating rate of 10  $\text{K min}^{-1}$  and with a dwelling time of 1 h. The sample and measurement cell were allowed to cool down to room temperature (assisted by water cooling) prior to conducting the  $\text{CO}_2$  sorption measurements. In the second part 10%  $\text{CO}_2$  was added to the gas stream for 30 min and purged subsequently with pure Ar for 2 h to remove residual gas-phase  $\text{CO}_2$ . In the third part a thermal treatment similar to the pre-treatment procedure was applied resulting in a temperature programmed desorption experiment of the adsorbed  $\text{CO}_2$ .

Pure anatase (99.5%, 10–25 nm, CAS Nr: [1317-70-0], IoLi-Tec) and commercially available  $\text{TiO}_2$  (P25, 99.5%, 21 nm, CAS Nr: [13463-67-7], Evonik) were used as sorption materials.

## Results

Fig. 1(i)–(iv) depict difference spectra recorded during different steps of the  $\text{CO}_2$  adsorption experiment (adsorption, purging, desorption) as described in the Experimental section. Difference spectra were selected to illustrate the changes in the features appearing during the measurements more clearly. Furthermore, this removes the effect of slight changes in the baseline prior to recording the spectra during adsorption. The corresponding (non-difference) spectra can be found in the ESI† (Fig. S5 for anatase and Fig. S6 for P25, ESI†). A Table with literature references to the vibrational bands of the different  $\text{CO}_2$ -derived surface species can also be found in the ESI† (Table S1).

Fig. 1(i) presents the difference spectra recorded during the  $\text{CO}_2$  adsorption experiment on anatase in the dark. It must be noted that despite the pretreatment, three prominent bands are already present before  $\text{CO}_2$  adsorption starts. They are located at  $\sim 1621$ , 1342 and 1269  $\text{cm}^{-1}$  (Fig. S5(i), ESI†). The band at 1621  $\text{cm}^{-1}$  is commonly assigned to the scissoring vibration of adsorbed molecular water.<sup>8</sup> The other two bands cannot be clearly assigned: Any definite assignment to a species containing C=O, OCO and C–OH functional groups (carbonate, bicarbonate, carboxylate, *e.g.*, acetate, formate...) would require the observation of at least one band in the range of  $\sim 1650$  to 1500  $\text{cm}^{-1}$ ,<sup>9,10</sup> potentially also accompanied by C–H bands, which are not observed. It is also not possible to assume another band hidden below the band of adsorbed water, because after the measurement (Fig. S5(ii), ESI†) adsorbed water is gone, but the bands at  $\sim 1345$  and 1269  $\text{cm}^{-1}$  are still present. We tentatively assign these bands to a CO(H) group, but without definite assignment to a particular species. Throughout the  $\text{CO}_2$  desorption experiment the intensity of the feature at 1346  $\text{cm}^{-1}$  decreases and its peak position shifts to 1324  $\text{cm}^{-1}$ . It is well known that increased coverage of the surface may lead to blue shifts of the corresponding feature in the IR spectrum.<sup>11,12</sup> Here, the decrease in intensity indicates a lower amount of this species upon  $\text{CO}_2$  adsorption, possibly because it interacts with or is

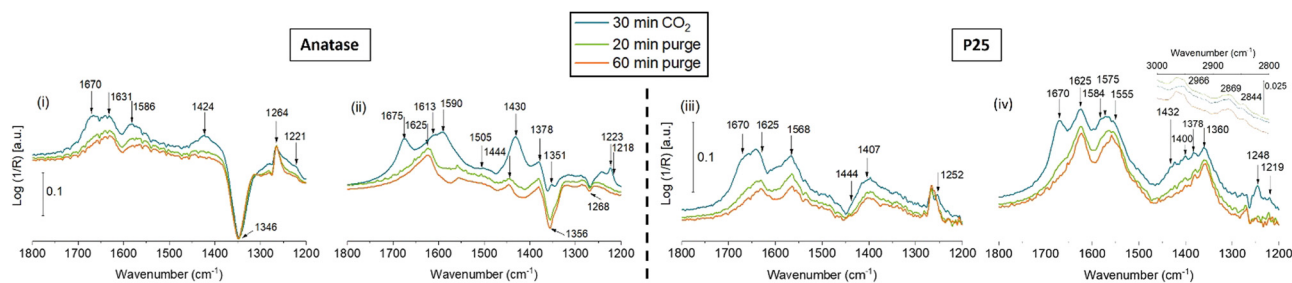


Fig. 1 Difference DRIFT spectra recorded during the  $\text{CO}_2$  adsorption experiment for anatase ((i) dark conditions, (ii) under illumination) and P25 ((iii) dark conditions, (iv) under illumination).



transformed by the adsorbates formed from CO<sub>2</sub>. Consequently, the coverage-dependent effect is reversed leading to a red shift of the feature back to lower wavenumbers.

Upon CO<sub>2</sub> adsorption (Fig. 1(i)) weak features are formed at 1670 and 1424 cm<sup>-1</sup> as well as 1221 cm<sup>-1</sup>. A broad band at 1631 cm<sup>-1</sup>, which is already present in the beginning of the measurement, might simply result from changes in the amount or structure of adsorbed water.<sup>8</sup> The newly arising bands at 1670, 1424 and 1221 cm<sup>-1</sup> can be assigned to bicarbonates.<sup>9,10,13</sup> According to ref. 4, this bicarbonate is monodentate. It cannot be unambiguously excluded that minor amounts of bidentate bicarbonates are also formed, because these species might share the band at ~1220 cm<sup>-1</sup>, whereas the  $\nu_{\text{as}}(\text{OCO})$  band at ~1623 cm<sup>-1</sup>, as well as the  $\nu_{\text{s}}(\text{CO})$  band at ~1440 cm<sup>-1</sup> (ref. 10) might be hidden below other bands. Another weak band arises at 1586 cm<sup>-1</sup>. It might be assigned to the additional formation of mono-<sup>9</sup> or bidentate<sup>10</sup> carbonate species. A reliable assignment to the band at 1586 cm<sup>-1</sup> to the  $\nu_{\text{as}}(\text{OCO})$  vibration of any carbonate requires the observation of the  $\nu_{\text{s}}(\text{OCO})$  band as a second feature. It may be suggested that additional bands contribute to the shoulders of the broad signals around 1424 and ~1220 cm<sup>-1</sup>. But no bands are clearly visible, making it impossible to unambiguously decide on the presence of additional carbonates.

As soon as CO<sub>2</sub> is removed from the gas feed and slowly purged out of the reaction chamber, monodentate bicarbonates are being desorbed, causing the corresponding features to decrease. They disappear almost entirely already at room temperature, whereas the band at 1631 cm<sup>-1</sup>, assigned to adsorbed water, is still visible. During the thermal treatment (Fig. S5, ESI†) features at 1345 and 1269 cm<sup>-1</sup> show a reverse behavior compared to the CO<sub>2</sub> adsorption and desorption step. At the end of the thermal treatment all adsorbed water seems to have been removed, causing a disappearance of the band around 1630 cm<sup>-1</sup>.

Fig. 1(ii) shows the DRIFT spectra of the CO<sub>2</sub> desorption, after light-assisted CO<sub>2</sub> adsorption. Strong features at 1675, 1430, 1223 and 1218 cm<sup>-1</sup> indicate the formation of mono- and bidentate bicarbonates,<sup>9,10,13</sup> similar to the dark experiment. But in the case of adsorption under irradiation, an additional species, identified by prominent positive features at 1590 and 1378 cm<sup>-1</sup>, is also formed. These species have been identified differently in previous works, ranging from monodentate carbonates<sup>9</sup> to bidentate carbonates<sup>9</sup> and carboxylates.<sup>13</sup> Rather similar bands were also observed upon CO<sub>2</sub> adsorption on TiO<sub>2</sub> disks with preferential (001) orientation, but they were assigned to two different species (1570 cm<sup>-1</sup>: carboxylate, 1390 cm<sup>-1</sup>: bicarbonate).<sup>14</sup> It should be noted here that the term “carboxylate” requires a more detailed discussion. Details are given in the ESI.† In brief, the correct use of the term carboxylate would refer to species such as formate or acetate, *i.e.*, containing a COO group. Previous works, however, named a simple COO<sup>-</sup> or COOH species as carboxylate, which can only be formed at electron-donating defect sites (such as Ti<sup>3+</sup>).<sup>10</sup> Some articles used the term without assigning any structure. Here, we assume that such species might originate from a bent

CO<sub>2</sub> species interacting with a proton, for example from a surface hydroxyl group, so that a structure between a bent CO<sub>2</sub> and a carboxylic acid function arises. For a lack of better options, and in agreement with previous works, we keep the name “carboxylate”, but both structure and name should be clarified in future works, for example with the assistance of surface science or computational chemistry.

Since these particular carboxyl species or carboxylates are usually only assigned when an additional band above 1650 cm<sup>-1</sup> is observed,<sup>7,10,15</sup> we exclude this assignment for the observed bands formed on anatase, but we cannot clearly differentiate between a mono- and a bidentate carbonate. A chelating bidentate bicarbonate species can also be assumed to be present, as weak shoulders at 1613 and 1505 cm<sup>-1</sup> can be seen in the spectrum.<sup>9</sup> In addition, a strong negative feature appears around 1355 cm<sup>-1</sup>. However, unlike the measurement of CO<sub>2</sub> adsorption in the dark (Fig. 1(i)), this signal features two bands: one increasingly negative feature at 1356 cm<sup>-1</sup> and a weaker positive one at 1351 cm<sup>-1</sup>. Different literature sources assign different vibrational modes to signals in this region. In general, a feature at around 1355 cm<sup>-1</sup> has been previously assigned to  $\nu_{\text{s}}(\text{OCO})$  in monodentate carbonates,<sup>14,16</sup> or  $\nu_{\text{s}}(\text{CO})$  in carboxylates.<sup>13</sup> As argued above, the presence of a carboxylate is unlikely here, so we tentatively assign this band to a mono- or bidentate carbonate, too. Moreover, it is suggested that the negative signal originates from a spectator species which is covered or converted during the adsorption experiment.

When CO<sub>2</sub> is removed from the atmosphere, carbonates seem to be desorbed, as the corresponding features disappear in the spectrum. However, several bands remain visible, such as signals at 1625, 1444 and which indicate the presence of stable bridging bidentate bicarbonate species.<sup>9,10</sup> This species might have been formed in presence of CO<sub>2</sub> already, however the characteristic features contributed to the strong signals dominated by monodentate species and were thus not clearly visible. This species is not formed in the dark experiment. Only labile species were formed in the dark, which were completely removed during room temperature purging.

The experiments with the anatase sample have been repeated with the mixed-phase material P25. Fig. 1(iii) shows DRIFT spectra recorded during the CO<sub>2</sub> adsorption and desorption steps on thermally pretreated P25 material in the dark. Raw spectra of the measurement (Fig. S6(i), ESI†) indicate the presence of some residual carbonate species after the pre-treatment, and prior to CO<sub>2</sub> adsorption. This includes the unidentified species with a band at 1267 cm<sup>-1</sup>, also present from the beginning on the pure anatase, and a band at 1444 cm<sup>-1</sup>. As will be discussed later, this band does not correspond to any other band in the spectrum. The band around 1625 cm<sup>-1</sup> again originated from adsorbed water.

When CO<sub>2</sub> was introduced into the reaction cell, bands appeared at 1670, 1625, 1568, ~1400 and 1252 cm<sup>-1</sup>. Here, the development of bands at 1670 and 1252 cm<sup>-1</sup>, clearly without the presence of additional bands at ~1424 and ~1220 cm<sup>-1</sup>, indicates the formation of the particular carboxylate,<sup>10,15</sup> or carboxyl species (bent CO<sub>2</sub> interacting with



a proton, see  $\text{ESI}^\dagger$ ), as has been observed in previous works with P25.<sup>7</sup> The strong band that appears around  $1568\text{ cm}^{-1}$  is attributed to  $\nu_{\text{as}}(\text{OCO})$  in monodentate carbonate.<sup>7,9</sup> The corresponding  $\nu_{\text{s}}(\text{OCO})$  is assumed to be part of the broad band around  $1400\text{ cm}^{-1}$ . The band at  $1625\text{ cm}^{-1}$ , this time not observed in correspondence with any other band, likely relates to changes in the adsorbed water.

DRIFT spectra of the subsequent purging indicate the desorption or decomposition of the carboxyl species, associated with the disappearance of the bands at  $1670$  and  $1252\text{ cm}^{-1}$ . The species with bands at  $1568$  and  $1400\text{ cm}^{-1}$ , likely a monodentate carbonate species, proves to be more stable, because it cannot be removed at room temperature. It can be removed during thermal treatment (Fig. S6(iii),  $\text{ESI}^\dagger$ ). In addition, the increase of the band at  $1269\text{ cm}^{-1}$  might indicate relative changes in the unidentified surface adsorbate, present from the beginning. In addition, as can be seen in the raw spectra of the thermal post-treatment (Fig. S6(iii),  $\text{ESI}^\dagger$ ), the only two bands left after sample treatment at  $400\text{ }^\circ\text{C}$  are located at  $1444\text{ cm}^{-1}$  and  $1269\text{ cm}^{-1}$ . This proves that the band at  $1444\text{ cm}^{-1}$  is not related to the band at  $1625\text{ cm}^{-1}$  or any other band.

The results of the  $\text{CO}_2$  adsorption experiment conducted under illumination with P25 are presented in Fig. 1(iv). The surface of this sample was much cleaner after the thermal pretreatment, as much less signals are apparent in the initial spectra (Fig. S6(ii),  $\text{ESI}^\dagger$ ). The band at  $1444\text{ cm}^{-1}$  was not visible here. The cleaner surface might be the reason for the overall higher intensity of the bands of the difference spectra, when compared to the spectra in Fig. 1(iii).

Features at  $1670$  and  $1248\text{ cm}^{-1}$  are again assigned to a carboxylate species. As these bands disappear during purging of the reaction cell with Ar, this undermines the assumption of weakly bound species. Monodentate carbonates are detected more clearly than in the dark experiment, with a feature at  $1575\text{ cm}^{-1}$  as well as the corresponding feature at  $1378\text{ cm}^{-1}$ . Additional features at  $1432$  and  $1219\text{ cm}^{-1}$  indicate the formation of bicarbonates, but a clear assignment to mono- or bidentate species is again not possible, as the distinguishing bands at either  $1670\text{ cm}^{-1}$  (monodentate) or  $1625\text{ cm}^{-1}$  (bidentate) are hidden below other bands.

So far, all species have been observed previously in the other measurements. But when irradiating P25 during  $\text{CO}_2$  adsorption, additional bands occur at  $1584$ ,  $\sim 1400$  and  $1360\text{ cm}^{-1}$ . These bands correspond rather well to the  $\nu_{\text{as}}(\text{OCO})$ ,  $\delta(\text{CH})$  and  $\nu_{\text{s}}(\text{OCO})$  of adsorbed formate species on rutile.<sup>17</sup> The band at  $1555\text{ cm}^{-1}$  might indicate the formation of another formate species, because bands at  $1558$  and  $1359\text{ cm}^{-1}$  have been assigned to formate species on P25.<sup>13</sup> It has been suggested previously that the bands slightly shift due to changes in the anatase-to-rutile ratio, or the degree or reduction of the surface.<sup>18</sup> It is important to note, however, that the unambiguous identification of formate species crucially relies on the simultaneous identification of the C–H stretch, which is expected between  $2800$  and  $3000\text{ cm}^{-1}$  (see inset of Fig. 1(iv)). Three weak features are apparent at around  $2966$ ,  $2869$  and  $2844\text{ cm}^{-1}$  which are characteristic for CH stretching vibrations in adsorbed formates.<sup>13,17–19</sup> Therefore,

formation of adsorbed formate species is strongly suggested. Tables S1 and S2 ( $\text{ESI}^\dagger$ ) provide a summary of the vibrational modes and identified species formed during the adsorption of  $\text{CO}_2$  on anatase and P25 in the dark or under illumination.

The results obtained in this study indicate that the types of (bi)carbonate species formed on the surface of  $\text{TiO}_2$  differ, depending on whether the sample was irradiated during  $\text{CO}_2$  adsorption. In both cases, the variety of species was larger under irradiation. DRIFTS is not a quantitative technique, but the different band heights relative to each other suggest also differing amounts of species. For the pure anatase, a mono- or bidentate carbonate species ( $1590$  and  $1378\text{ cm}^{-1}$ ) has been clearly observed during  $\text{CO}_2$  adsorption under irradiation, whereas only a very small band at  $1590\text{ cm}^{-1}$  was seen in the dark experiment. This hints at a relatively larger surface coverage when  $\text{CO}_2$  is adsorbed with irradiation. In this case, chelating bidentate bicarbonate species ( $1613$  and  $1505\text{ cm}^{-1}$ ) were also present, that were not seen in the dark experiment. In addition, during desorption, stable bridging bidentate bicarbonate species ( $1625$  and  $1444\text{ cm}^{-1}$ ) were only found after  $\text{CO}_2$  adsorption under irradiation, not after the dark experiment.

Using P25 as photocatalyst, regardless of irradiation, species ( $1670$  and  $1251\text{ cm}^{-1}$ ) are formed that have previously been named as carboxylate, but may rather resemble a carboxylic acid function. These species were not seen in the experiment with anatase. A potential important role of such carboxylate species in photocatalytic  $\text{CO}_2$  reduction has been suggested previously.<sup>7,16</sup> When the formation of the carboxylate is suppressed in sodium-modified P25, the activity in  $\text{CO}_2$  reduction dropped.<sup>7</sup>

Formate species ( $2966$ ,  $2869$ ,  $2844$ ,  $1584$ ,  $1555$ ,  $\sim 1400$  and  $1360\text{ cm}^{-1}$ ) were formed only on P25, and only during irradiation, which may be seen as proof of the first step of successful  $\text{CO}_2$  reduction. Caution is advised here: It may be stoichiometric reaction, involving co-adsorbates such as those present after the pretreatment, or hydroxyl groups. Future operando DRIFTS studies must be performed to clarify this question. Bicarbonate species ( $1432$  and  $1219\text{ cm}^{-1}$ ; bands above  $1600\text{ cm}^{-1}$  hidden) on P25 were also clearly identified only after irradiation, indicating that light enabled their formation, or favored the formation of larger amounts.

The reasons behind these observations must be further clarified in future, but it indicates that irradiation already majorly influences the very first elementary steps, which are the adsorption equilibria of reactants.

## Conclusions

The influence of UV illumination on  $\text{CO}_2$  adsorption on anatase and P25 was investigated qualitatively by means of DRIFTS. While on anatase illumination was found to cause more intense bands of more stable carbonate and bicarbonate surface species, respectively, on P25 additional bicarbonate and formate species were formed. The observations might be a first step towards explaining pathways and bottlenecks in the activation and reaction of  $\text{CO}_2$ .



## Author contributions

P. N.: investigation, formal analysis, methodology, writing – original draft, writing – review & editing. N. G. M.: methodology, validation, writing – original draft, writing – review & editing. M. K.: resources, methodology, writing – review & editing. T. P.: resources, supervision, writing – review & editing. J. S.: conceptualization, writing – review & editing, funding acquisition, supervision.

## Data availability

The authors confirm that the data supporting the findings of this study are available within the article and the ESI.†

## Conflicts of interest

There are no conflicts to declare.

## Acknowledgements

The authors acknowledge financial support by the Leibniz-Program Cooperative Excellence K308/2020 (project “SUPREME”). Part of this research was funded by the German Ministry of Education and Research (BMBF) within the scope of the funding program CO2WIN (033RC024, project “PRODIGY”).

## References

- 1 Y. Cao, M. Yu, S. Qi, T. Wang, S. Huang, Z. Ren, S. Yan, S. Hu and M. Xu, *Phys. Chem. Chem. Phys.*, 2017, **19**, 31267–31273.
- 2 M. A. Henderson, *Surf. Sci.*, 1998, **400**, 203–219.
- 3 S. N. Habisreutinger, L. Schmidt-Mende and J. K. Stolarczyk, *Angew. Chem., Int. Ed.*, 2013, **52**, 7372–7408.
- 4 T. Luttrell, S. Halpegamage, J. Tao, A. Kramer, E. Sutter and M. Batzill, *Sci. Rep.*, 2014, **4**, 4043.
- 5 W. He, J. Xiong, Z. Tang, Y. Wang, X. Wang, H. Xu, Z. Zhao, J. Liu and Y. Wei, *Appl. Catal., B*, 2024, **344**, 123651.
- 6 L. Zhang, Q. Zhao, L. Shen, Q. Li, T. Liu, L. Hou and J. Yang, *Catal. Sci. Technol.*, 2022, **12**, 509–518.
- 7 A. Pougin, M. Dilla and J. Strunk, *Phys. Chem. Chem. Phys.*, 2016, **18**, 10809–10817.
- 8 M. Takeuchi, L. Bertinetti, G. Martra, S. Coluccia and M. Anpo, *Appl. Catal., A*, 2006, **307**, 13–20.
- 9 L. Mino, G. Spoto and A. M. Ferrari, *J. Phys. Chem. C*, 2014, **118**, 25016–25026.
- 10 J. Baltrusaitis, J. Schuttlefield, E. Zeitler and V. H. Grassian, *Chem. Eng. J.*, 2011, **170**, 471–481.
- 11 W. F. Lin, M. S. Zei, M. Eiswirth, G. Ertl, T. Iwasita and W. Vielstich, *J. Phys. Chem. B*, 1999, **103**, 6968–6977.
- 12 W. F. Lin, P. A. Christensen, A. Hamnett, M. S. Zei and G. Ertl, *J. Phys. Chem. B*, 2000, **104**, 6642–6652.
- 13 K. K. Bando, K. Sayama, H. Kusama, K. Okabe and H. Arakawa, *Appl. Catal., A*, 1997, **165**, 391–409.
- 14 U. Tumuluri, J. D. Howe, W. P. Mounfield, M. Li, M. Chi, Z. D. Hood, K. S. Walton, D. S. Sholl, S. Dai and Z. Wu, *ACS Sustainable Chem. Eng.*, 2017, **5**, 9295–9306.
- 15 W. Wu, K. Bhattacharyya, K. Gray and E. Weitz, *J. Phys. Chem. C*, 2013, **117**, 20643–20655.
- 16 K. Bhattacharyya, A. Danon, B. K. Vijayan, K. A. Gray, P. C. Stair and E. Weitz, *J. Phys. Chem. C*, 2013, **117**, 12661–12678.
- 17 R. P. Groff and W. H. Manogue, *J. Catal.*, 1983, **79**, 462–465.
- 18 M.-Y. He, J. M. White and J. G. Ekerdt, *J. Mol. Catal.*, 1985, **30**, 415–430.
- 19 G. Y. Popova, T. V. Andrushkevich, Y. A. Chesalov and E. S. Stoyanov, *Kinet. Catal.*, 2000, **41**, 805–811.

